Influence of envelope geometry on the sensitivity of ''nude'' ionization gauges

Albert R. Filippelli[a)]
Thermophysics Division, Chemical Science and Technology Laboratory, National Institute of Standards and Technology, Gaithersburg, Maryland 20899

(Received 28 March 1996; accepted 21 June 1996)

This article presents the results of some measurements of the influence of envelope size and shape on the N_2 sensitivity of two nominally identical ''nude'' extractor ionization gauges, and three common ''nude'' versions of the Bayard–Alpert ionization gauge. Measurements were made over the pressure range 10^{-7}–10^{-1} Pa, using typical gauge operating parameters and with vacuum chamber and gauge envelope at ground potential. Sensitivity values corresponding to the three different envelopes used in this work differed by as much as a factor of 2 (comparing maximum value to minimum value for each gauge) for the Bayard–Alpert gauges. For the extractor gauges, the differences were as large as 7%.

I. INTRODUCTION

In addition to a dependence on the values of its emission current and bias voltages, it has long been established that the sensitivity of an ionization gauge will also depend on the size, position, and relative spacing of the gauge's component parts, including the envelope that surrounds the gauge (see, for example, Refs. 1–7). However, the practical implications of these facts, in particular, the influence of the envelope, may not be widely known among users of ionization gauges. Unfamiliarity with the influence of the envelope can be attributed in part to the fact that very often the envelope is an integral part of the gauge structure. For example, the ordinary triode gauge and the very popular Bayard–Alpert gauge are quite commonly built with a glass envelope. In some glass-envelope versions of these gauges a thin conductive layer (usually platinum) held fixed at filament potential is deposited on the inner glass surface. For either the coated or uncoated glass envelope, the dimensions and the relative spacing of the envelope and gauge structure are not altered by the user. In this case, there exists a nominal or average sensitivity value for the gauge (assuming manufacturing tolerances are maintained and operating parameters are specified, including the potential of the inner surface of the envelope[8]). However, for a ''nude'' version of a gauge (i.e., constructed on a vacuum flange without any envelope) the envelope is defined by the size, shape, and potential of the port in which the gauge is mounted. Thus, the sensitivity of a nude gauge will be somewhat dependent on the way it is mounted on the system. This is not new knowledge, but there may not be a widespread appreciation of its significance among current users of nude gauges. Further, there is a lack of published quantitative information concerning this effect that can be readily applied by users of nude gauges, and an apparent lack of recognition of its importance when manufacturers specify sensitivity for nude gauges. The purpose of this article is to illustrate the magnitude of the effect that envelope size/shape can have on a nude gauge's sensitivity.

[a)]Electronic mail: afilip@enh.nist.gov

II. EXPERIMENTAL SETUP

Three commercially available nude Bayard–Alpert gauges, identified as **BAG 1**, **BAG 2**, and **BAG 3**, were used in this experiment. These BAGs have similar dimensions (see Table I) and each employs a ''closed cage'' grid constructed of small diameter wire (intended for electron-bombardment degassing only). The experiment also included two (nominally identical) commercially available nude extractor gauges, identified as **EXG 1** and **EXG 2**. Each gauge is built on a standard 70 mm copper gasket-sealed stainless steel ultrahigh vacuum (UHV) flange (ConFlat®, Varian Associates, Palo Alto, CA or other manufacturers' equivalents). Hereafter, we use the term ''CF'' to refer to this type of flange. The nominal vendor-specified sensitivity to N_2 for these gauges is given in the last column of Table I. The gauges and calibration chamber were not subjected to any degassing procedure other than baking at 250 °C for about 12 h before each data set.

Gauge bias voltages and emission currents (see Table I) were set at or close to recommended values. The chamber and all vacuum plumbing hardware were always at ground potential. Each gauge was operated with a commercial controller dedicated to that gauge throughout the experiment. The three BAG controllers were nominally identical as were the two EXG controllers. Five high quality electrometers, each one dedicated to a particular gauge throughout the experiment, were used to measure the gauges' collector currents.

III. PROCEDURE

Each gauge's absolute N_2 sensitivity[9] was determined in each of three envelope configurations, designated **A**, **B**, and **C**, and shown in Fig. 1. In configuration **A**, a gauge was mounted directly into one of the 70 mm CF ports of the calibration chamber. The port's flange is joined to the wall of the 457-mm-diam cylindrical calibration chamber by a 25 mm length of 35-mm-i.d. tubing. For mounting configuration **B**, a 114–70 mm adapter flange was used to mount a gauge into one of the chamber's 114 mm CF ports. These larger

TABLE I. Operating parameters and dimensional information for the gauges.

Gauge	Grid Diam (mm)	Grid Length (mm)	Grid Bias (V)	Filament Material	Filament Length (mm)	Filament Distance from grid axis (mm)	Filament Bias (V)	Filament Emission (mA)	Ion collector Bias (V)	Specified sensitivity (Pa^{-1}) [$Torr^{-1}$]
BAG 1	20	45	188	ThO_2–Ir	36	13	30	1	0	(0.19) [25]
BAG 2	20	45	185	W	33	13	32	1	0	(0.19) [25]
BAG 3	23	43	184	W	30	13	30	1	0	(0.19) [25]
EXG 1	13	25	233	ThO_2–Ir	57[a]	9	96	1.4	0	(0.05) [6.7]
EXG 2	13	25	219	ThO_2–Ir	57[a]	9	87	1.5	0	(0.05) [6.7]

[a]The filament is a circular loop, centered on the grid axis, and with the plane of loop parallel to the flange face.

ports are joined to the chamber wall by a 25 mm length of 60-mm-i.d. tubing. In configuration **C**, a gauge was mounted inside a 102 mm long×35-mm-i.d. nipple attached to a 70 mm CF port. Configuration **C** provided the least nude environment for the Bayard–Alpert gauges. For each gauge, the envelope was the only parameter that was changed from one set of measurements to the next. The gauges were operated simultaneously, although they were not all in the same mounting configuration at the same time. For example, in the first set of measurements, **BAG 1**, **BAG 2**, **BAG 3**, **EXG 1**, and **EXG 2** were in mounting configurations **C**, **C**, **B**, **A**, and **A**, respectively. Calibration pressure values were generated with the National Institute of Standards and Technology (NIST) primary vacuum standard[10] or were measured with a spinning rotor gauge[11–13] that had been calibrated *in situ* against the primary standard.

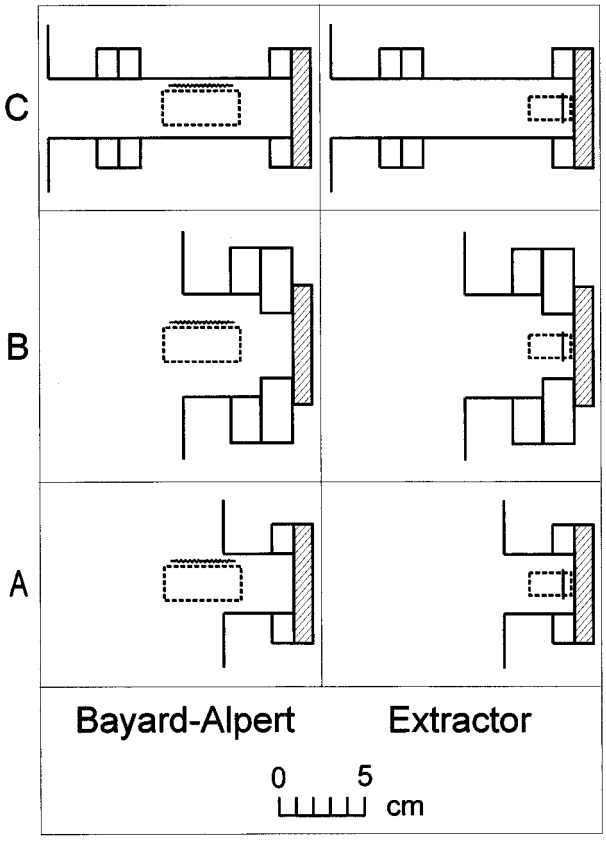

FIG. 1. Scale drawing showing size and location of the gauges relative to the calibration chamber ports for the three mounting configurations used in this experiment. A gauge's 70 mm CF flange is shown shaded in this drawing. The heavy dashed line rectangle represents a gauge's grid. For the BAGs, the wavy line next to the grid represents the filament. The circular loop filament for the EXGs is represented by the short heavy line parallel to the flange face. Grid-to-flange distance shown for the BAGs (31 mm) applies to **BAG 2** and **BAG 3**. For **BAG 1**, this distance was 28 mm.

IV. RESULTS

Figure 2 shows the sensitivity results for each gauge in each configuration plotted on a linear scale versus pressure on a logarithmic scale. Absolute sensitivity determinations were made in all cases, but Fig. 2 presents these results in normalized form. Each gauge's absolute sensitivity results have been divided by that gauge's sensitivity at 10^{-4} Pa in the configuration that gave the largest overall sensitivity (configuration **C** for the BAGs, and configuration **B** for the EXGs). At the time they were determined, the normalizing divisor values (given in Table II) had an estimated 2σ uncertainty of about 0.7%.

At the end of the experiment, long-term stability of three of the gauges (**BAG 1**, **BAG 2**, and **EXG 1**) was checked by returning them to their original configurations (**C**, **C**, and **A**, respectively) and repeating the measurement of their sensitivities. This was not possible for gauges **BAG 3** and **EXG 2** since they were not available at every stage of the experiment. These repeated sensitivity measurements for gauges **BAG 1**, **BAG 2**, and **EXG 1** agreed with the corresponding original measurements to within 7%, 1%, and 1%, respectively. For overall clarity in the graphs, these repeat results are not shown in Fig. 2. Although we have been unable to identify a particular reason for the relatively poor repeatability of the measurements in the case of **BAG 1** (comparing

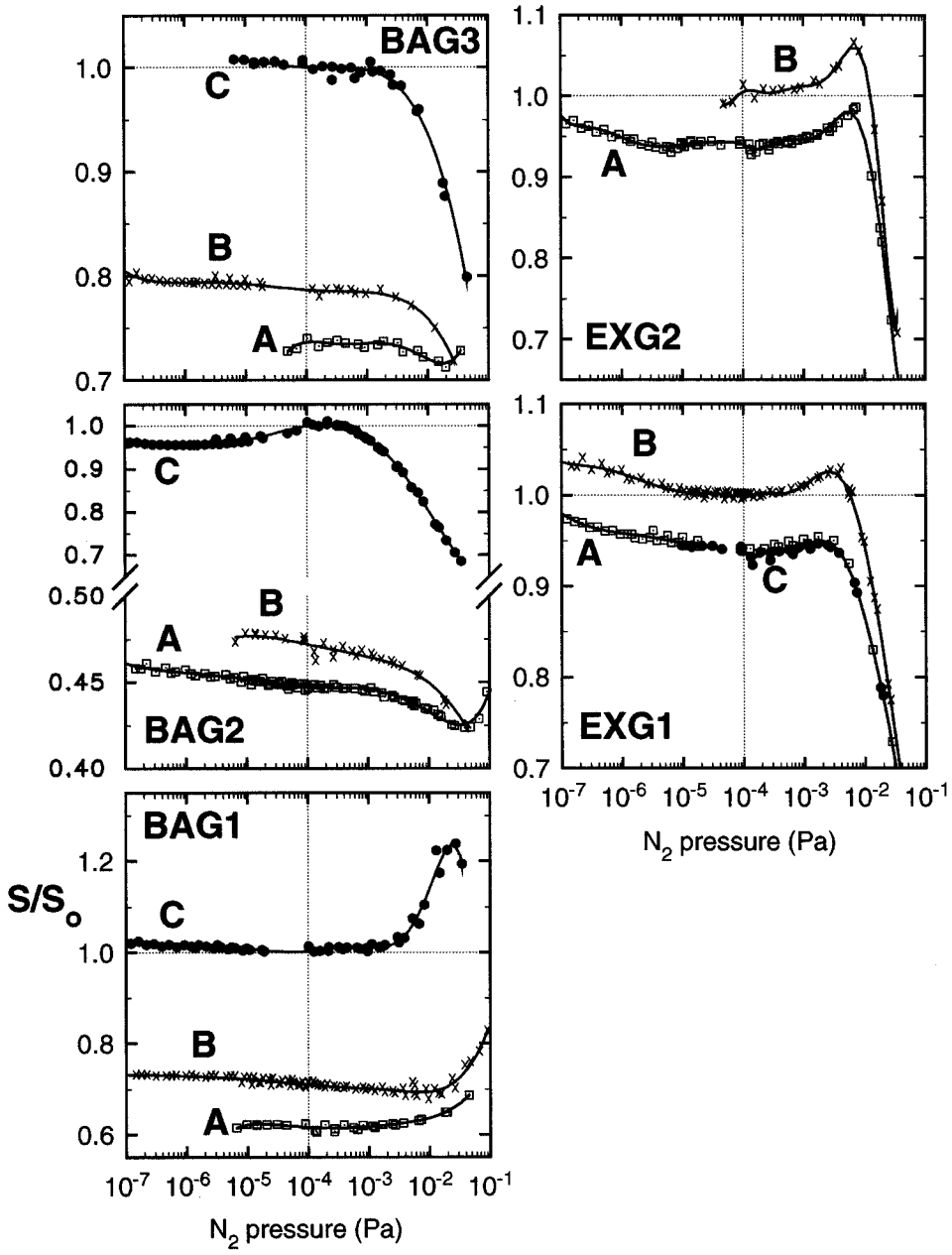

FIG. 2. Normalized N_2 sensitivity results. For each BAG, the normalizing divisor was chosen as the measured sensitivity of that gauge in mounting configuration **C** at a calibration pressure of 1×10^{-4} Pa, and for the EXGs, the measured sensitivity in configuration **B** at 1×10^{-4} Pa. These normalizing divisors are given in Table II.

original and final results obtained in configuration **C**), this behavior is not inconsistent with our earlier experience with BAGs with ThO_2–Ir filaments.[14]

A. Bayard–Alpert gauges

Although the pressure dependence of the sensitivity differs in detail for all three BAGs, the normalized sensitivities have the same ordering for all three gauges: for each gauge, the highest sensitivity was obtained in the least nude configuration **C**, an intermediate value was obtained for configuration **B**, and lowest sensitivity was obtained in configuration **A**. At 10^{-4} Pa, the sensitivity of **BAG 1**, **BAG 2**, and **BAG 3** in configuration **B** was roughly 70%, 47%, and 80%, re-

TABLE II. Measured sensitivity at 10^{-4} Pa. These are the normalizing divisors used to generate the normalized results presented in Fig. 2.

		Sensitivity to N_2 determined in this work at 10^{-4} Pa	
Gauge	Configuration	(Pa^{-1})	($Torr^{-1}$)
BAG 1	**C**	0.129	17.1
BAG 2	**C**	0.237	31.6
BAG 3	**C**	0.182	24.3
EXG 1	**B**	0.0695	9.26
EXG 2	**B**	0.0658	8.77

spectively, of the sensitivity in configuration **C**. In configuration **A**, these values were, respectively, about 60%, 45%, and 73% of the corresponding configuration **C** values. Comparison of the normalizing divisor values given in Table II for the BAGs with the corresponding vendor-specified nominal sensitivity values in Table I shows that the absolute sensitivity obtained in configuration **C** for the BAGs is closest in magnitude to the vendor-specified nominal value. The sensitivity values obtained for **BAG 1**, **BAG 2**, and **BAG 3** in configuration **C** at 10^{-4} Pa (see Table II) lie within +27% and −32% of the vendor-specified nominal value (25 Torr^{-1}) for these BAGs. The average (24.3 Torr^{-1}) of these three values lies within 3% of this nominal value.

B. Extractor gauges

Of the three tested configurations, both EXGs showed largest sensitivity in configuration **B**. In configurations **A** and **C** there is no significant difference between the results obtained for **EXG 1** since there is no real difference between these two mounting arrangements (refer to Fig. 2). **EXG 2** was not available for measurements in configuration **C**. At 10^{-4} Pa, the sensitivity of both EXGs in configuration **A** was about 93% of the corresponding sensitivity in configuration **B** (refer to Table II for the absolute value of sensitivity in configuration **B** at 10^{-4} Pa). Closest agreement between the measured absolute N_2 sensitivities at 10^{-4} Pa and the vendor-specified nominal value (0.05 Pa^{-1}) was found in configuration **A** (and **C** for **EXG 1**, and presumably also for **EXG 2**). However, the less-than-maximum absolute sensitivity values obtained in configurations **A** (and **C**) were still about 29% and 22% *larger* than the nominal value for **EXG 1** and **EXG 2**, respectively.

Because the overall length of the grid structure for the EXG is about half that for the BAGs, and because this grid structure is mounted much closer to the CF flange than for the BAGs, the wall in case **B** for most of the EXG structure was defined by the hole in the adapter flange (refer to Fig. 1). The diameter (38 mm) of this hole is slightly *larger* than the wall diameter (35 mm) seen by the EXG in cases **A** and **C**. Thus, unlike the BAGs, largest sensitivity for the EXGs was obtained with a more nude mounting of the gauges.

V. DISCUSSION

A. Modeling of Bayard–Alpert gauges

The gauge modeling work of Redhead[3] and of Pittaway,[4] provides physical insight into the cause of the observed changes of BAG sensitivity with envelope size. They represented the grid, collector, and surrounding wall as very long cylindrical concentric equipotential surfaces, and the filament as a long straight wire parallel to the gauge axis. In a (ρ,θ,z) cylindrical polar coordinate system in which the gauge's axis is coincident with the z axis, the electric potential in the gauge then depends only on ρ and θ, and is independent of z. The potential, V_F, of the filament is in general held at some value intermediate between the potentials V_G and V_W of the grid and the wall, respectively. That is, $V_G > V_F > V_W$. One important result that emerged from the modeling is that, for given grid, filament, and wall radii, ρ_G, ρ_F, and ρ_W, and given grid and filament potentials, V_G and V_F, the gauge's sensitivity could be maximized for a particular value of the wall potential V_W. This particular value of wall potential is the one for which the resulting potential at the location $\rho=\rho_F$ *in the absence of the filament* is equal to the actual filament potential. By choosing this particular wall potential, the distortion in the vicinity of the filament of the otherwise radial electric field is minimized, and electron trajectories follow mostly radial paths into and through the grid volume. Both Redhead and Pittaway concluded that, for a given geometry and grid–filament potential difference, the sensitivity would be maximized for this particular wall potential because the electron path length inside the grid space would be maximized.

Conversely, for the case in which the potentials V_G, V_F, and V_W are fixed, as well as ρ_G and ρ_F (as in an actual gauge), we should be able to make the radius of the undisturbed equipotential surface at filament potential match the radius to the actual filament location by adjusting the diameter of the tubing surrounding the gauge structure. The gauge modeling results suggest that, as a result, the sensitivity would then be maximized. In the present experiment, three wall diameters were employed, corresponding to the three mounting arrangements **A**, **B**, and **C**. (For case **A**, the wall was considered to have infinite radius for the BAGs; for cases **B** and **C**, the wall radii were 30 and 17.5 mm, respectively.) Using the values given in Table I for the gauge dimensions and potentials, and using the simple modeling of the gauge in which the potential $V(\rho)$ between the grid and the wall varies as

$$V(\rho)=V_G-(V_G-V_W)\left(\frac{\ln\left(\frac{\rho}{\rho_G}\right)}{\ln\left(\frac{\rho_W}{\rho_G}\right)}\right), \tag{1}$$

the unperturbed potential (volts) at the filament location $\rho=\rho_F$ corresponding to cases **A**, **B**, and **C** are 188, 143, and 100 V for **BAG 1**; 185, 141, and 98 V for **BAG 2**; 184, 134, and 69 V for **BAG 3**. As the radius of the surrounding tube is made smaller (going from case **A** to case **C**), the calculated value of the unperturbed potential at the location of the filament approaches the actual filament potential. The expectation of a corresponding sequence of increasing sensitivity values is qualitatively in agreement with the measurement results presented in this article. The model yields the following values for the wall radius ρ'_W for which the unperturbed potential at the filament location will be equal to the actual filament potential: ρ'_W = 13.7, 13.7, and 13.3 mm, respectively, for **BAG 1**, **BAG 2**, and **BAG 3**. Thus, for this model calculation, a sensitivity maximum would be achieved when the wall of the surrounding tube was less than 1 mm from the filament.

B. Envelope influence on nonlinearity

Nonlinearity is the deviation of a gauge's sensitivity from a constant value as the pressure is varied. Figure 2 shows that all the tested gauges exhibited some nonlinearity. (1) In the case of the EXGs, the change in sensitivity with envelope size (comparing results for configuration **B**, with **A** or **C**) can be characterized by a simple pressure-independent scaling over the entire 1×10^{-7}–4×10^{-2} Pa range of this investigation. That is, for the EXGs the degree of nonlinearity was not changed when the envelope dimensions were changed. (2) For **BAG 1** and **BAG 3**, the effect of changing the envelope size is characterized by a pressure-independent scaling of the sensitivity for pressures below about 10^{-3} Pa. Above this pressure, the nonlinearity was different for each mounting configuration. For **BAG 2** envelope size influenced the gauge's nonlinearity for pressures above about 10^{-5} Pa.

VI. SUMMARY

For absolute pressure measurement with an ion gauge, one must know the absolute sensitivity of the gauge or the calibration factor for the gauge/controller system. Even if the desired information is just the relative dependence of some quantity on pressure, one still must at least know the relative dependence of the gauge's sensitivity on pressure. The results presented in this article show that when the dimensions of a gauge's envelope are changed there can be a significant change in the absolute magnitude of the gauge's sensitivity. There may also be a change in the relative dependence of its sensitivity on pressure. If these changes are not taken into account, the accuracy and self-consistency of pressure measurements made with the gauge will be adversely affected. These results show that, if the gauge envelope is different from the one in which it has been calibrated, pressure measurement errors as large as 50% are possible with some BAGs. Errors as large as about 7% are possible with the EXG. Even if one were making only relative measurements, the influence of the envelope could lead to an apparent disagreement between pressure measurements made at two locations with the same gauge. Thus, the envelope must be considered a proper part of an ionization gauge, and a specification of ''nude'' gauge sensitivity is incomplete unless the geometry and potential of the envelope are also given.

[1]J. J. Kinsella, in *Vacuum Symposium Transactions* (1954), pp. 65–68.
[2]J. Groszkowski, Proceedings of the Third International Congress on Vacuum Techniques, 28 June–2 July 1965, Stuttgart, Germany, in *Advances in Vacuum Science and Technology* (Pergamon, London, 1967), Vol. 2, Part 1, pp. 241–244.
[3]P. A. Redhead, J. Vac. Sci. Technol. **6**, 848 (1969).
[4]L. G. Pittaway, J. Phys. D: Appl. Phys. **3**, 1113 (1970).
[5]P. C. Arnold and D. G. Bills, J. Vac. Sci. Technol. A **2**, 159 (1984).
[6]H. C. Hseuh and C. Lanni, J. Vac. Sci. Technol. A **5**, 3244 (1987).
[7]D. G. Bills, J. Vac. Sci. Technol. A **12**, 574 (1994).
[8]In the case of a BAG operated with ac heating current for the filament and with an *un*coated glass envelope, the potential of the inner surface of the envelope can depend on pressure. For a discussion of how the filament potential wave form can influence the pressure dependence of the wall potential, see, for example, P. J. Abbott and J. P. Looney, J. Vac. Sci. Technol. A **12**, 2911 (1994).
[9]The sensitivity S was calculated as $S=[I_c-I_{c0}]/[(P-P_0)I_{\rm em}]$ where I_c is a gauge's collector current at total pressure $P=P_0+\Delta P$, I_{c0} is its collector current at the base pressure P_0 in the calibration system, $I_{\rm em}$ is the gauge's electron emission current, and ΔP is the calibration pressure.
[10]This standard is geometrically similar to, but somewhat larger than, the primary high vacuum standard that was described by C. R. Tilford, S. Dittmann, and K. E. McCulloh in J. Vac. Sci. Technol. A **6**, 2853 (1988), and S. Dittmann, in *The High Vacuum Standard and Its Use*, NIST Special Publication 250-34 (NIST, Gaithersburg, MD, 1989).
[11]J. K. Fremerey, Vacuum **32**, 685 (1982).
[12]J. K. Fremerey, J. Vac. Sci. Technol. A **3**, 1715 (1985).
[13]S. Dittmann, B. E. Lindenau, and C. R. Tilford, J. Vac. Sci. Technol. A **7**, 3356 (1989).
[14]A. R. Filippelli and P. J. Abbott, J. Vac. Sci. Technol. A **13**, 2582 (1995).